HSPB7 is indispensable for heart development by modulating actin filament assembly

Tongbin Wu[a], Yongxin Mu[a], Julius Bogomolovas[a,b], Xi Fang[a], Jennifer Veevers[a], Roberta B. Nowak[c], Christopher T. Pappas[d], Carol C. Gregorio[d], Sylvia M. Evans[a,e], Velia M. Fowler[c], and Ju Chen[a,1]

[a]Department of Medicine, School of Medicine, University of California, San Diego, La Jolla, CA 92093; [b]Department of Cognitive and Clinical Neuroscience, Central Institute of Mental Health, Medical Faculty Mannheim, Heidelberg University, Mannheim 68159, Germany; [c]Department of Molecular Medicine, The Scripps Research Institute, La Jolla, CA 92037; [d]Department of Cellular and Molecular Medicine, University of Arizona, Tucson, AZ 85721; and [e]Skaggs School of Pharmacy, University of California, San Diego, La Jolla, CA 92093

Edited by Vann Bennett, Duke University Medical Center, Durham, NC, and approved September 25, 2017 (received for review August 4, 2017)

Small heat shock protein HSPB7 is highly expressed in the heart. Several mutations within HSPB7 are associated with dilated cardiomyopathy and heart failure in human patients. However, the precise role of HSPB7 in the heart is still unclear. In this study, we generated global as well as cardiac-specific HSPB7 KO mouse models and found that loss of HSPB7 globally or specifically in cardiomyocytes resulted in embryonic lethality before embryonic day 12.5. Using biochemical and cell culture assays, we identified HSPB7 as an actin filament length regulator that repressed actin polymerization by binding to monomeric actin. Consistent with HSPB7's inhibitory effects on actin polymerization, HSPB7 KO mice had longer actin/thin filaments and developed abnormal actin filament bundles within sarcomeres that interconnected Z lines and were cross-linked by α-actinin. In addition, loss of HSPB7 resulted in up-regulation of Lmod2 expression and mislocalization of Tmod1. Furthermore, crossing HSPB7 null mice into an Lmod2 null background rescued the elongated thin filament phenotype of HSPB7 KOs, but double KO mice still exhibited formation of abnormal actin bundles and early embryonic lethality. These in vivo findings indicated that abnormal actin bundles, not elongated thin filament length, were the cause of embryonic lethality in HSPB7 KOs. Our findings showed an unsuspected and critical role for a specific small heat shock protein in directly modulating actin thin filament length in cardiac muscle by binding monomeric actin and limiting its availability for polymerization.

HSPB7 | heart development | sarcomere | thin filament assembly | actin polymerization

Several cardiac disease-causing mutations have been found within thin filament genes, such as *ACTC1* (1), *TPM1*, and *TNNT2* (2), reinforcing the realization that the proper function of cardiac muscle relies on precise regulation of thin filament contractile function. A critical characteristic of thin filaments is their tightly controlled length, which is closely related to specific contractile properties of distinct striated muscle types (3, 4). Several actin binding proteins regulate thin filament length. The pointed end capping protein tropomodulin 1 (Tmod1) (5) limits thin filament length by inhibiting addition of actin to the pointed end of actin filaments (6, 7). The actin nucleator, leiomodin2 (Lmod2) (8), is also required for regulating thin filament length in cardiac muscle, as mice lacking Lmod2 exhibit shorter filament lengths and reduced force-generating ability in cardiac myocytes (9). The importance of precise regulation of thin filament length is shown by the subsequent development of dilated cardiomyopathy in Lmod2 mutants (9) or in transgenic (Tg) mice overexpressing Tmod1 in their hearts (10). Moreover, loss of Lmod3, the Lmod gene expressed predominantly in skeletal muscle, results in severe nemaline myopathy characterized by sarcomere disorganization and shorter thin filaments in both humans and mice (11, 12). However, whether there are additional regulators that contribute to this process and how actin binding proteins work in concert to tightly regulate thin filament length remain largely unknown.

Small heat shock proteins (sHSPs) are a family of molecular chaperones that bind nonnative proteins to prevent their aggregation and assist in subsequent refolding by ATP-dependent chaperones, such as HSP70 (13), or in targeting unfolded proteins for degradation by proteasomal and/or autophagic pathways. While some sHSPs are ubiquitously expressed, others are relatively confined to heart and skeletal muscle, including HSPB6 and HSPB7 (14). sHSPs recognize a broad spectrum of substrates, ranging from cytoskeletal proteins to mitochondrial proteins (13). Interestingly, sHSPs also associate with the actin cytoskeleton (15). In addition, HSPB5/αB-crystallin is known to stabilize filamentous actin (16), while HSPB1 was originally purified from turkey smooth muscle as a fraction that inhibits actin polymerization (17). However, mechanisms by which sHSPs directly modulate actin dynamics await additional investigation.

HSPB7 (also known as cardiovascular HSP) is highly expressed in heart and skeletal muscle (18). Mutations found within the HSPB7 gene are associated with heart disease (19–22). In zebrafish, loss-of-function studies showed that HSPB7 is essential for left–right asymmetry and cardiac morphogenesis (23, 24). However, the role of HSPB7 in mammalian heart is still unclear. To further investigate biological functions of HSPB7, we generated mice with global KO of HPSB7 and found that they died from heart defects before embryonic day 12.5 (E12.5). Close examination of sarcomeres in KO cardiomyocytes revealed the presence of abnormal actin bundles (AABs), which were continuous

Significance

Sarcomeres, the contractile units of striated muscle, are composed of thick and thin/actin filaments. Thin filament length is closely associated with specific contractile properties of individual muscles, and it is tightly controlled by actin binding proteins. However, it is still unclear how these proteins work in concert to maintain proper thin filament length and whether there are additional factors involved. In this study, we found that deleting HSPB7 resulted in uncontrolled elongation of actin filaments and the formation of atypical actin filament bundles in cardiomyocytes. Biochemical studies revealed a previously unsuspected function of HSPB7 in interacting with and limiting actin monomer availability for actin filament polymerization, giving mechanistic insight into the etiology of aberrant sarcomeres observed in HSPB7 null heart.

Author contributions: T.W., S.M.E., V.M.F., and J.C. designed research; T.W., Y.M., J.B., X.F., and R.B.N. performed research; R.B.N., C.T.P., C.C.G., and V.M.F. contributed new reagents/analytic tools; T.W., Y.M., J.B., X.F., R.B.N., V.M.F., and J.C. analyzed data; and T.W., J.V., C.C.G., S.M.E., V.M.F., and J.C. wrote the paper.

The authors declare no conflict of interest.

This article is a PNAS Direct Submission.

[1]To whom correspondence should be addressed. Email: juchen@ucsd.edu.

This article contains supporting information online at www.pnas.org/lookup/suppl/doi:10.1073/pnas.1713763114/-/DCSupplemental.

throughout the length of the sarcomere and associated with α-actinin. Measurement of thin filament length revealed longer thin filaments, which coincided with up-regulation of the actin binding protein Lmod2. However, genetic ablation of Lmod2 in HSPB7 KO embryos did not prevent formation of AABs, although average thin filament lengths were reduced, consistent with deletion of Lmod2 alone (9). The foregoing suggests that up-regulation of Lmod2 was important for increased thin filament length but not for assembly of AABs in HSPB7 mutants. Interestingly, we found that HSPB7 bound to monomeric actin (G actin) and repressed actin polymerization, indicating that loss of HSPB7 could result in excessive actin polymerization and AAB formation. Our findings shed light on HSPB7's role in thin filament length regulation and suggest a possible interplay between HSPB7 and regulators, such as Lmod2 and Tmod1.

Results

HSPB7 Is Essential for Fetal Heart Development. To investigate HSPB7's function in vivo, we generated an HSPB7 KO mouse line utilizing homologous recombination. In brief, Exon 2 of the HSPB7 gene was flanked by two LoxP sites, and a neomycin cassette was inserted immediately downstream in Intron 2 to serve as a selection marker (Fig. S1*A*). Correctly targeted ES cells were used to generate living mice via germ-line transmission and bred with ubiquitously expressed Sox2-Cre (25) mice to generate an HSPB7 global KO allele. Western blot results from E11.5 hearts of KO animals indicated complete loss of HSPB7 protein (Fig. S1*A*). We were unable to recover viable KOs, suggesting that HSPB7 KO mice died in utero (Fig. S1*B* and Table S1). From E9.5 to E10.5, mutants were grossly indistinguishable from WT littermates (Fig. 1*A*). However, at E11.5, mutants had noticeably smaller left ventricles compared with WT littermates (Fig. 1*A*). Examination of embryonic hearts revealed that HSPB7 KO embryos had relatively smaller hearts, starting from E10.5 (Fig. S1*C*). We also observed enlargement of cardinal veins in E10.5 KO embryos by PECAM (platelet endothelial cell adhesion molecule) staining (Fig. S1*D*), an indication of congestive heart failure (26). At E11.5, nearly one-half of KO embryos had died and begun to be resorbed, and by E12.5, most HSPB7 KO embryos had died (Fig. S1*B* and Table S1).

To uncover detailed morphological changes in mutant hearts, we performed H&E staining on embryonic heart sections. At E10.5, HSPB7 KO hearts were slightly smaller and more rounded in shape relative to controls (Fig. S1*E*). By E11.5, trabeculae were smaller and thinner, and the right ventricular wall was thinner in E11.5 mutant hearts relative to controls (Fig. 1*B*). To investigate whether the observed phenotypes were owing to loss of HSPB7 function in cardiomyocytes, we examined expression of HSPB7 by whole-mount RNA in situ hybridization of WT and mutant embryos. Results showed that HSPB7 was exclusively expressed in heart and undetectable in other parts of the embryo (Fig. S2*A*). Immunofluorescent staining using antibodies against HSPB7 and the cardiomyocyte marker α-actinin indicated that that HSPB7 expression was confined to cardiomyocytes (Fig. S2*B*). HSPB7 was expressed throughout the cytoplasm of cardiomyocytes in an irregular punctate pattern in contrast to the striated pattern observed for sarcomeric α-actinin (Fig. S2*B*). To further ensure that observed phenotypes resulted from a cardiomyocyte-specific requirement for HSPB7, we used Nkx2.5-Cre (27) and cTnT-Cre (28) mouse lines to delete HSPB7 specifically in cardiomyocytes. Timed pregnancy results showed that all HSPB7 cardiac-specific KO (cKO) embryos developed similar phenotypes as global KO embryos, similarly dying before E12.5 (Fig. S2*C* and Tables S2 and S3).

As expression of HSPB7 was confined to cardiomyocytes (Fig. S2 *A* and *B*) and the overall phenotype of cKOs resembled those of global KOs (Fig. 1*B* and Fig. S2*C*), we decided to use the global HSPB7 KO for the remainder of our experiments. To investigate whether a decrease in cardiomyocyte proliferation could account for smaller hearts and thinner trabeculae in mutant embryos, we used antibodies against the mitotic marker Phospho-Histone H3 (pHH3) and sarcomeric α-actinin to highlight proliferative cardiomyocytes (Fig. S2*D*). Quantification of the percentage of pHH3-positive cardiomyocytes indicated that proliferation in HSPB7 KO was not affected until E11.5 (Fig. S2*E*), when about 40% of mutant embryos had already died. Decreased proliferation observed at this stage just before death suggested that it might be a secondary event rather than causative for the observed phenotype. We barely observed apoptotic cardiomyocytes in both WT and HSPB7 KO E9.5–E11.5 embryos by Cleaved Caspase 3 staining (Fig. S2*F*).

AABs Form Within Sarcomeres of HSPB7 KO Cardiomyocytes. Sarcomeres are the fundamental unit of the contractile apparatus in cardiomyocytes. Interestingly, sHSPs translocate to and stabilize sarcomeres under stress conditions (29). We, therefore, asked whether there were defects in sarcomere assembly that might lead to insufficient cardiac function in HSPB7 KO embryos. To assess sarcomere integrity, we performed immunofluorescence staining of E11.5 embryonic heart sections using antibodies against two classic sarcomeric proteins: α-actinin at the Z line and myomesin at the M line. In WT cardiomyocytes, Z lines and M lines were prominent and discrete, indicating proper assembly of sarcomeres (Fig. 2*A*). On the contrary, sarcomeres in HSPB7 KO cardiomyocytes were poorly organized (Fig. 2*A*). Whereas M lines were relatively unchanged, Z lines were narrower and had a "checkerboard" appearance. Of note, there were atypical structures interconnecting Z lines that were stained by both α-actinin (Z line) and phalloidin (F actin) (yellow arrows in Fig. 2*A*), indicating that they were actin filaments associated with α-actinin. Similar abnormal structures were observed in E9.5 KO hearts and E10.5 KO hearts (yellow arrows in Fig. S3*A*), indicating that this phenomenon preceded emergence of an overt cardiac morphogenetic phenotype. As the abnormal structures could be stained by phalloidin and contained α-actinin, we designated them AABs. To further characterize AABs, we used antibodies against another Z-line protein, cypher (30, 31), to investigate whether cypher also might be a component of AABs. As shown in Fig. S3*B*, cypher staining was detected in most AABs marked by α-actinin (yellow arrows in Fig. S3*B*). We also used an antibody that specifically recognizes the Z-line portion of titin (Z1Z2) to examine whether titin was included in AABs. Although the Z-line portion of titin was largely overlapping with α-actinin in both WT and mutant sarcomeres, the great majority of AABs did not contain Z1Z2 of titin (yellow arrows in Fig. S3*C*). In very rare instances, Z1Z2 was observed within AABs (yellow arrowheads in Fig. S3*C*).

Troponin–tropomyosin complexes are pivotal to contractile function of sarcomeres (32). To investigate whether AABs possessed troponin–tropomyosin complexes and might have the potential to contract, we used two antibodies against Tpm1 (Fig.

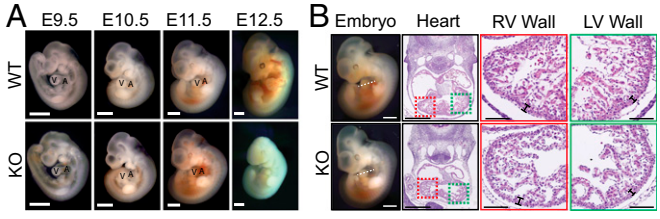

Fig. 1. General phenotype of HSPB7 KO mice. (*A*) Images of WT and KO embryos from E9.5 to E12.5. A, left atria; V, left ventricle. (Scale bar: 1 mm.) (*B*) H&E images of E11.5 embryos acquired using NanoZoomer slide scanner. (Scale bar: 0.5 mm.) Estimated location of sectioning is indicated by a dotted line on the whole-mount embryos images, *Left*. (Scale bar: 1 mm.) Magnified right ventricle (RV; red box) and left ventricle (LV; green box) wall views are shown, *Right*. Left and right ventricle wall thicknesses are indicated by rulers. (Scale bar: 0.1 mm.)

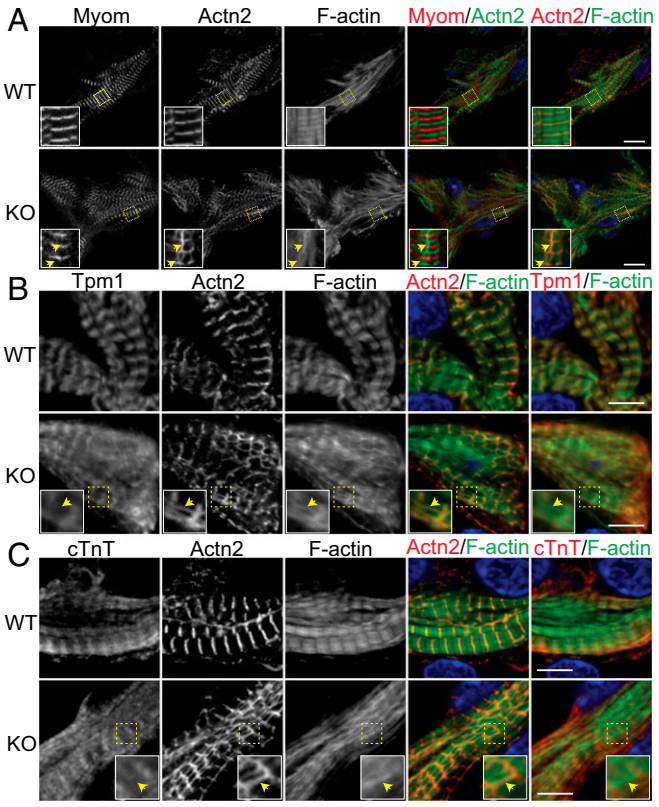

Fig. 2. Characterization of AABs in HSPB7 KO embryos. (*A*–*C*) WT and KO heart cryosections were stained with phalloidin (F actin) and antibodies against α-actinin (Actn2) and (*A*) E11.5: Myomesin (Myom), (*B*) E10.5: Tpm1, or (*C*) E10.5: cTnT. The locations of AABs or their relative positions are indicated by yellow arrows. High magnification views are shown as *Insets* in corresponding images. Colors are depicted in merged images. DNA is stained with DAPI (blue). (Scale bar: *A*, 10 μm; *B* and *C*, 5 μm. Magnification: *A*, *Insets*, 3.3×; *B* and *C*, *Insets*, 2.2×.)

2*B*) and cardiac troponin T (cTnT) (Fig. 2*C*). As expected, the staining pattern of Tpm1 or cTnT appeared closely flanking the Z lines, consistent with staining of the narrow cardiac I bands. However, neither Tpm1 nor cTnT were detected in AABs (yellow arrows in Fig. 2 *B* and *C*). This result indicated that AABs did not contain troponin–tropomyosin complexes and thus, would be unlikely to generate contractions. Moreover, neither myomesin nor myosin heavy chain were detected in the AABs, also indicating that they are noncontractile (Fig. 2*A* and Fig. S3*D*).

Desmin forms short filament-like structures interconnecting Z lines (33). We found similar desmin-containing structures in both WT and mutant cardiomyocytes (green arrows in Fig. S3*E*), but they did not overlap with AABs (red arrows in Fig. S3*E*), indicating that they are distinct from AABs. Because HSPB7 has been reported to interact with filamin C (Flnc) to prevent its aggregation and mislocalization (34), we also performed immunostaining with antibodies to Flnc. However, no changes in localization of Flnc and no evidence for Flnc aggregates were observed in mutant cardiomyocytes. Additionally, Flnc was not observed within AABs (yellow arrows in Fig. S3*F*).

Taken together, AABs found in HSPB7 KO cardiomyocytes appear to be an abnormal form of actin filaments bundles that lack a troponin–tropomyosin complex but include the Z-line components α-actinin and cypher (Fig. S3*G*). Formation of AABs appears to reflect defective actin filament/thin filament assembly, as no alterations were observed in thick filaments based on immunostaining for myomesin (Fig. 2*A*) and myosin heavy chain (Fig. S3*D*).

HSPB7 KO Hearts Have Increased Lmod2 and Longer Thin Filaments in Their Sarcomeres. The foregoing observations suggested that thin filament assembly was dysregulated in HSPB7 KO hearts. As thin filament assembly is a highly regulated process involving a myriad of actin binding proteins (35), we examined the abundance of various key regulators of actin dynamics under the assumption that HSPB7 might stabilize one or some of these proteins acting as a molecular chaperone. While amounts of most candidate proteins remain unchanged, the actin nucleator Lmod2 was significantly up-regulated in HSPB7 KO hearts (Fig. 3*A* and Fig. S4 *A*–*C*). The intermediate filament protein desmin was also up-regulated (Fig. S4 *B* and *C*), although this might be a secondary effect, as its level increases in heart failure (36). Interestingly, qRT-PCR analyses showed that Lmod2 mRNA levels exhibited a similar fold increase to that of Lmod2 protein (two- to threefold) (Fig. S4 *D* and *E*). This observation suggested that HSPB7 might not directly regulate levels of Lmod2 through a protein–protein interaction.

In a previous study, overexpression of Lmod2 in cultured cardiomyocytes reduced binding of the pointed end capping protein Tmod1 to pointed ends of actin filament, and was accompanied by thin filament elongation (37). As Lmod2 was significantly up-regulated in HSPB7 KO hearts, we assessed thin filament length in both WT and HSPB7 KO cardiomyocytes. Thin filament length was significantly increased in HSPB7 KO cardiomyocytes from E10.5 hearts (Fig. 3*B*), reminiscent of findings in Lmod2-overexpressing cardiomyocytes (37). Although overall amounts of the pointed end capping protein Tmod1 were unchanged (Fig. 3*A* and Fig. S4*A*), and some Tmod1 was associated with thin filament pointed ends in the middle of the sarcomere, another portion of Tmod1 appeared diffusely localized throughout the cytoplasm in the HSPB7 KO cardiomyocytes (Fig. 3*C*). This contrasts with WT sarcomeres, where all of the Tmod1 is located at the thin filament pointed ends and no cytoplasmic Tmod1 is detected (Fig. 3*C*). This suggests that not all Tmod1 had assembled at its normal sarcomeric location in the absence of HSPB7, consistent with defects in thin filament assembly. Reduced Tmod1 capping of thin filament pointed ends may contribute to their elongation (38).

Loss of HSPB7 Leads to Formation of AABs Independent of Lmod2 and Tmod1. Lmod2 KO mouse cardiomyocytes have shorter thin filament lengths, and mice develop early-onset dilated cardiomyopathy (9). Thus, if abnormal elongation of thin filaments was

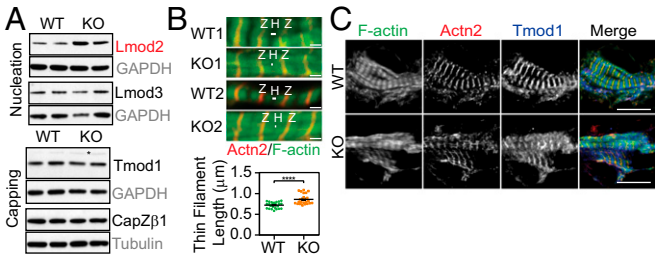

Fig. 3. Lmod2 is up-regulated, and thin filament length is increased in HSPB7 KO embryos. (*A*) Western blots of various thin filament length regulators in E11.5 hearts isolated from WT and KO. GAPDH or α-tubulin served as loading controls (gray). Proteins depicted in red were found to be significantly increased in HSPB7 KO embryos. Asterisk in Tmod1 indicates nonspecific bands. (*B*) Immunofluorescence images (*Upper*) of two (1, 2) WT and KO embryos from E10.5 heart sections. Z lines were stained using antibodies against α-actinin (Actn2; red), and actin (thin) filaments were stained using phalloidin (green). Quantification of WT vs. HSPB7 KO thin filament length (*Lower*). Two embryos and 12–20 sarcomeres per group. Error bars indicate mean ± SEM. Statistical significance was determined with two-tailed Student's *t* test. H, actin-free H zone; Z, Z lines. ****$P < 0.0001$. (Scale bar, 1 μm.) (*C*) WT and HSPB7 KO E10.5 heart cryosections were stained with phalloidin (F actin) and antibodies against Actn2 and Tmod1. (Scale bar: 10 μm.)

caused by elevated expression of Lmod2, we hypothesized that depletion of Lmod2 in HSPB7 KO mice might ameliorate sarcomeric defects. To address this, we generated Lmod2/HSPB7 double-homozygous null mice. Immunofluorescent staining using antibodies against HSPB7 and Lmod2 indicated that both proteins were successfully eliminated in double-KO embryos (Fig. S5*A*), which died before E12.5, the same stage as HSPB7 KOs. As expected, thin filament length was reduced ∼9% in Lmod2 KO cardiomyocytes (9) and increased ∼4% in HSPB7 KOs (Fig. S5*B*). The average thin filament length observed in Lmod2 KOs was incrementally increased by ∼4% by loss of HSPB7, comparable with that observed in HSPB7 KOs alone. These observations suggested that each of these pathways regulates thin filament length in an opposite and independent fashion. Examination of thin filament assembly by performing immunostaining with sarcomeric α-actinin antibody and phalloidin showed that AABs were still present in double-KO embryos (yellow arrowheads in Fig. S5*C*). Together, these observations indicated that sarcomeric phenotypes observed in HSPB7 KOs could not be rescued by loss of Lmod2, and thus, were not consequent to observed up-regulation of Lmod2. These results indicate that HSPB7 directly limits thin filament length and that loss of HSPB7 leads to AAB formation by an Lmod2-independent pathway.

The presence of Tmod1 in the cytoplasm of HSPB7 KO cardiomyocytes could have resulted from the up-regulation of Lmod2, as Tmod1 and Lmod2 have been proposed to compete for binding to pointed ends in cultured cardiomyocytes (37). However, the presence of cytoplasmic Tmod1 was not corrected in Lmod2/HSPB7 double-KO embryos (Tmod1 staining in Fig. S5*C*), suggesting that alterations in Tmod1 localization were not caused by up-regulation of Lmod2. Previous studies in cultured cardiomyocytes have shown that inhibition of Tmod1 activity by antibody microinjection results in actin filament elongation from pointed ends, with increased overall length of thin filaments, and decreased beating of cardiomyocytes (38). These observations suggested that reduced Tmod1 association with thin filament pointed ends could potentially account for the increased length of sarcomeric actin filaments and/or formation of AABs in HSPB7 KO embryos. Therefore, to examine whether overexpression of Tmod1 could rescue HSPB7 phenotypes, we crossed Tmod1 Tg mice (10) into an HSPB7 KO background. Immunofluorescence images of whole embryonic hearts showed that expression of Tmod1 was substantially increased in Tmod1 Tg hearts and HSPB7 KO/Tmod1 Tg hearts (Fig. S6*A*). Despite the significant increase of Tmod1 at pointed ends (compare red arrowheads with green arrowheads in Fig. S6*B*), AABs were still present in HSPB7 KO/Tmod1 Tg embryonic hearts (yellow arrowheads in Fig. S6*B*). However, the thin filament length was not altered in HSPB7 KO/Tmod1 Tg compared with HSPB7 KO, although thin filaments were slightly shortened in Tmod1 Tg compared with WT (Fig. S6*C*). These results indicated that increasing Tmod1 at pointed ends could not rescue either the AAB or longer thin filament phenotype of the HSPB7 KOs.

HSPB7 Reduces Actin Polymerization by Directly Binding G Actin. The foregoing findings suggested that HSPB7 might directly influence actin polymerization independent of Lmod2 and Tmod1. To investigate mechanisms by which HSPB7 could affect actin polymerization, we sought to determine whether there was a direct interaction between HSPB7 and actin. To this end, we investigated whether HSPB7 bound to F actin using a cosedimentation binding assay. We observed that HSPB7 alone pelleted after ultracentrifugation (Fig. 4*A*), probably because of its tendency to form high-molecular weight oligomers (39). Interestingly, we found that the portion of HSPB7 in the supernatant fraction containing G actin increased when coincubated with F actin but not with BSA (Fig. 4*A*), while F-actin binding protein α-actinin-2 was coprecipitated with F actin (Fig. S7*A*). This result suggested that HSPB7 might bind directly to G actin rather than to F actin. To examine whether HSPB7 interacted with actin in

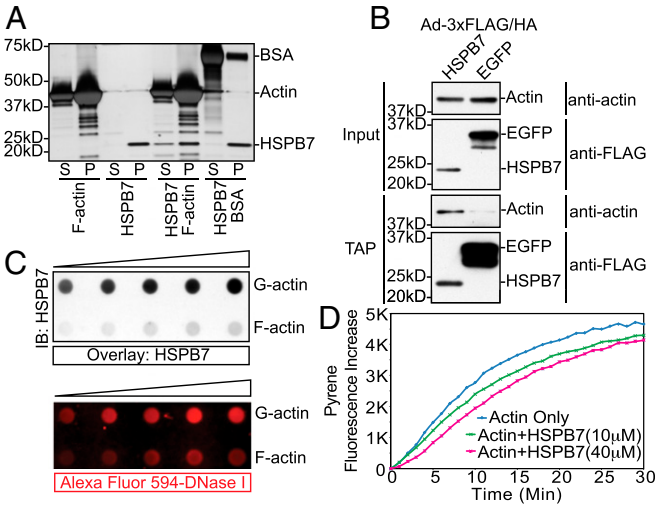

Fig. 4. HSPB7 binds G actin and inhibits actin polymerization. (*A*) Silver stain image of F-actin cosedimentation binding assay. S, supernatant; P, pellet. (*B*) TAP performed in isolated neonatal mouse cardiomyocytes infected by adenoviruses expressing either 3xFLAG/HA-tagged HSPB7 or EGFP. Samples were immunoblotted with actin or FLAG antibodies. The residual amount of actin in control EGFP sample is caused by unspecific binding of actin to EGFP, which was expressed at a much higher level than HSPB7. (*C*) Western blot image of blot overlay assay using an antibody against HSPB7 (*Upper*). Fluorescence image of Alexa Flour 594-conjugated DNase I incubated with the same membrane after treatment with stripping buffer (*Lower*). IB, immunoblot. (*D*) Actin polymerization assay with or without the presence of recombinant HSPB7 protein. Pyrene labeled G actin (2 μM) was preincubated with increasing amount of HSPB7 (10 μM, green; 40 μM, magenta) or buffer alone (blue).

mouse cardiomyocytes, we performed tandem affinity purification (TAP) using isolated neonatal mouse cardiomyocytes infected with adenovirus-expressing 3xFLAG/HA-tagged HSPB7. Results confirmed that the interaction between HSPB7 and actin occurred in cardiomyocytes (Fig. 4*B*). To investigate a direct interaction between HSPB7 and G actin, we utilized a blot overlay assay by immobilizing either G actin or F actin on Nitrocellulose membranes and then, overlaying with HSPB7 protein. Western blotting with antibody to HSPB7 indicated that HSPB7 preferentially bound G actin over F actin in a manner comparable with preferential binding of DNase I to G actin over F actin (40) (Fig. 4*C*). The much weaker binding of HSPB7 observed in F-actin samples was likely owing to the presence of some unpolymerized G actin within F-actin preparations (Fig. S7*B*). Interestingly, the interaction with G actin was a unique feature of HSPB7, as another heart-enriched sHSP, HSPB5/αB-crystallin, did not bind G actin in reciprocal blot overlay assays (Fig. S7*C*). To further confirm the interaction between G actin and HSPB7, we performed zero-length covalent cross-linking experiments using EDC [*N*-(3-dimethylaminopropyl)-*N*'-ethylcarbodiimide hydrochloride] and NHS (*N*-hydroxysuccinimide) (41, 42). Purified HSPB7 and G actin could be covalently cross-linked to a complex with a molecular mass of ∼65 kDa, consistent with a 1:1 stoichiometry of the HSPB7–actin complex (asterisks in Fig. S7*D*). Furthermore, both HSPB7 and actin were found within the complex as shown by Western blot analysis (asterisks in Fig. S7*D*). Taken together, our results showed that HSPB7 bound G actin both in vitro and in cardiomyocytes.

Next, we sought to determine whether HSPB7 was capable of inhibiting actin polymerization based on its ability to interact with G actin and thus, could have the potential to prevent excessive thin filament elongation in cells. To this end, we performed actin polymerization assays with or without purified recombinant HSPB7 protein. Interestingly, we found that HSPB7 seemed to reduce the rate of actin polymerization in a dose-dependent manner (Fig. 4*D*).

Like other actin binding proteins [e.g., profilin (43) and LATS1], we had to use relatively high concentrations of HSPB7 to repress actin polymerization. Taken together, these results suggest that HSPB7 may transiently bind G actin and limit its ability to polymerize.

Discussion

In this study, we have identified a role for an sHSP in regulating thin filament length in cardiomyocytes in vivo and elucidated the mechanism by which it does so. HSPB7-deficient embryos died before E12.5 and exhibited increased thin filament length and AABs that extended across the normally actin-free H zone. Although defects in cardiomyocyte proliferation were observed at E11.5 in HSPB7 KOs (Fig. S2*E*), proliferative defects are likely to be secondary to cardiac dysfunction and not causal to cardiac dysfunction, as they occurred at a time when 40% of the HSPB7 KO embryos had died; also, defects in cardiac muscle structure were already evident by E9.5 (Fig. S3*A*). We found that expression of the actin nucleator Lmod2 was up-regulated, and the pointed end capping protein Tmod1 was mislocalized in HSPB7 KOs, suggesting that dysregulation of these proteins might account for sarcomeric phenotypes of HSPB7 KOs. However, genetic rescue studies indicated that sarcomeric phenotypes of HSPB7 KOs were independent of dysregulation of Lmod2 or Tmod1, suggesting a more direct role for HSPB7 in regulating thin filament length. Indeed, several biochemical analyses showed that HSPB7 directly binds to monomeric G actin, which could reduce its ability to polymerize into F actin and thus, limit thin filament growth.

We found that average thin filament length was increased in HSPB7 KO embryos. As overexpression of Lmod2 tends to increase thin filament length (37), we sought to determine if up-regulation of Lmod2 in HSPB7 KO could account for the phenotypes by creating Lmod2/HSPB7 double-KO mice. Like Lmod2 single-KO mice (9), the thin filament length was significantly reduced compared with HSPB7 single KO, underscoring the importance of Lmod2 in maintaining proper thin filament length. Although it seemed that up-regulation of Lmod2 could explain the average thin filament length increase in HSPB7 KO, we found that thin filaments in Lmod2/HSPB7 double KO were still significantly longer than Lmod2 single KO, indicating that HSPB7 may directly repress thin filament elongation via a distinct pathway from Lmod2. Interestingly, the percentage of thin filament length increase in Lmod2/HSPB7 double KO over Lmod2 KO was comparable with the increase in HSPB7 KO over control, indicating that the loss of HSPB7's inhibitory effect, rather than increased expression of Lmod2, largely contributes to the longer thin filaments in the HSPB7 KO cardiomyocytes.

Overexpression of Lmod2 was thought to inhibit Tmod1's binding to pointed end by direct competition (37); however, recently, a new model has been proposed that Lmod overexpression and enhanced actin nucleation would generate more nascent thin filaments that elongate from their barbed ends. An increased number of filaments with free pointed ends could compete with preexisting pointed ends for limiting Tmod, resulting in decreased capping frequency and increased actin addition at pointed ends and longer filaments (44). Similarly, the up-regulation of Lmod2 observed in HSPB7 KO cardiomyocytes could produce excess free pointed ends with reduced Tmod1 capping, possibly contributing to the longer thin filaments observed in HSPB7 KO. To test this possibility, we overexpressed Tmod1 by crossing Tmod1 Tg mice to the HSPB7 KO background. However, an increased amount of Tmod1 at the pointed end did not reduce the length of the elongated thin filaments in HSPB7 KO, although thin filament length was decreased in Tmod1 Tg mice compared with WT as expected (10). This observation implies that thin filaments may largely elongate from their barbed ends in HSPB7 KO, as Tmod1 only inhibits addition of actin to the pointed end (6). Additionally, HSPB7 reduced rates of spontaneous actin polymerization in vitro, consistent with an effect on barbed ends, as polymerization occurs predominantly at fast-growing barbed ends under the conditions tested (45).

The AABs were continuous throughout the sarcomere. By probing with various antibodies raised against sarcomeric components, we discovered that these AABs bundles contain Z-line components, including α-actinin, but lack thin filament (Tpm1, cTnT) or thick filament components (myosin heavy chain, myomesin), which are critical for sarcomere contractile function (32). We concluded that these abnormal actin filament bundles are an aberrant Z-line structure and are unlikely to contract independently. We speculate that continued growth of thin filaments from their barbed ends through the H zone might result in confluence of antiparallel actin filaments, allowing binding of α-actinin and thus, mimicking the situation at the Z line (Fig. S8). Thus, α-actinin and other Z-line proteins (e.g., cypher) would recognize AABs as a pseudo-Z line. In addition, we found that expression of α-actinin remained constant in HSPB7 KO compared with WT (Fig. S4 *B* and *C*). The expansion of the abnormal Z-line structures containing α-actinin, F actin, cypher, and other Z-line components might decrease the amount of correctly localized α-actinin at the Z lines, which might further exacerbate defective thin filament assembly. The formation of these abnormal Z-line structures in HSPB7 KO cardiomyocytes resembles expanded Z-line pathologies referred to as streaming Z lines or nemaline bodies in skeletal muscle myopathies (46). To our knowledge, such structures have not been reported before in developing mouse cardiac muscles. Our data show that loss of the thin filament length regulator, Lmod2, in HSPB7 KOs does not rescue formation of AABs, implying that HSPB7 can act independently of Lmod2 in repressing excessive elongation of thin filaments and abnormal expansion of Z lines. Our data also suggest that the AABs, but not elongated thin filament length, may be the cause of cardiac defects and embryonic lethality in the HSPB7 KO mice. However, additional studies are needed to determine whether indeed AABs are sufficient to cause observed cardiac defects and lethality or whether the latter are caused by other as yet unidentified factors.

The mammalian sHSP family consists of 10 family members, HSPB1–10 (47). Although several sHSPs (e.g., HSPB5/αB-crystallin, HSPB6, HSPB7, and HSPB8) are relatively enriched in the heart (14), only ablating HSPB7 leads to an embryonic lethal phenotype in mice. In contrast, HSPB5/2 double-KO (48) and HSPB8-KO (49) mice are viable and do not have a basal cardiac phenotype. In addition, we recently showed that HSPB5, HSPB6, and HSPB8, which interact with BAG3, show a dramatic reduction in protein levels in Bag3 cardiac-specific KO mutant hearts (50). On the contrary, HSPB7, which does not interact with Bag3 (51), was unaltered (50). Together, these observations show that HSPB7 possesses an indispensable and unique function in the heart, which is distinct from other sHSPs. Our observation that, in contrast to HSPB7, αB-crystallin did not interact with G actin in blot overlay assays (Fig. S7*C*) also highlighted that the ability of HSPB7 to bind G actin and limit its availability for polymerization is not a common feature of sHSPs.

Recently, mice lacking HSPB7 specifically in skeletal muscle were reported to develop progressive myopathy (34). Flnc aggregation was found in HSPB7-deficient muscles, and the amount of Flnc aggregates was correlated with the severity of symptoms (34). However, we did not observe Flnc aggregation or any changes in Flnc localization in our HSPB7 KO embryos (Fig. S3*F*), indicating that HSPB7 may play different roles in cardiac and skeletal muscle. This notion was further supported by differences in HSPB7's subcellular localization in embryonic heart and skeletal muscle. We observed that HSPB7 was evenly distributed in E11.5 cardiomyocytes. In contrast, HSPB7 was found to localize at the Z line in skeletal muscle cells (34) and adult cardiomyocytes (52), implying that HSPB7 might play distinct roles in embryonic and adult cardiomyocytes. These findings also indicate that

HSPB7 could be involved in biological processes other than actin dynamics, which warrants additional investigation.

Materials and Methods

The sources of reagents and detailed methods are described in *SI Materials and Methods*. All animal studies were performed in accordance with the NIH *Guide for the Care and Use of Laboratory Animals* (53) and approved by the Institutional Animal Care and Use Committee of the University of California, San Diego. HSPB7 KO mice were generated as described (54). Immunostaining and in situ hybridization were performed as described (55, 56). qRT-PCR was performed as described (57). HSPB7 coding sequence was amplified from mouse adult heart cDNA and cloned into pET-trx1a (58).

ACKNOWLEDGMENTS. We thank Dr. Siegfried Labeit (University of Heidelberg) and Dr. Walter Witke (University of Bonn) for providing titin Z1Z2 antibody and cofilin1, respectively. J.B. is supported by European Commission Marie Skłodowska-Curie Individual Fellowship Titin Signals 656636. R.B.N. and V.M.F. are funded by NIH Grant HL083464. C.T.P. and C.C.G. are funded by NIH Grant HL123078. S.M.E. is supported by grants from the National Heart, Lung, and Blood Institute (NHLBI). V.M.F. and J.C. are supported by NIH Grant P30 AR061303. J.C. was funded by grants from the NHLBI and Foundation Leducq.

1. Olson TM, et al. (2000) Inherited and de novo mutations in the cardiac actin gene cause hypertrophic cardiomyopathy. *J Mol Cell Cardiol* 32:1687–1694.
2. Thierfelder L, et al. (1994) Alpha-tropomyosin and cardiac troponin T mutations cause familial hypertrophic cardiomyopathy: A disease of the sarcomere. *Cell* 77:701–712.
3. Gokhin DS, Bang ML, Zhang J, Chen J, Lieber RL (2009) Reduced thin filament length in nebulin-knockout skeletal muscle alters isometric contractile properties. *Am J Physiol Cell Physiol* 296:C1123–C1132.
4. Gokhin DS, Fowler VM (2013) A two-segment model for thin filament architecture in skeletal muscle. *Nat Rev Mol Cell Biol* 14:113–119.
5. Weber A, Pennise CR, Babcock GG, Fowler VM (1994) Tropomodulin caps the pointed ends of actin filaments. *J Cell Biol* 127:1627–1635.
6. Gokhin DS, Fowler VM (2011) Tropomodulin capping of actin filaments in striated muscle development and physiology. *J Biomed Biotechnol* 2011:103069.
7. Littlefield R, Almenar-Queralt A, Fowler VM (2001) Actin dynamics at pointed ends regulates thin filament length in striated muscle. *Nat Cell Biol* 3:544–551.
8. Chereau D, et al. (2008) Leiomodin is an actin filament nucleator in muscle cells. *Science* 320:239–243.
9. Pappas CT, et al. (2015) Knockout of Lmod2 results in shorter thin filaments followed by dilated cardiomyopathy and juvenile lethality. *Proc Natl Acad Sci USA* 112:13573–13578.
10. Sussman MA, et al. (1998) Myofibril degeneration caused by tropomodulin overexpression leads to dilated cardiomyopathy in juvenile mice. *J Clin Invest* 101:51–61.
11. Yuen M, et al. (2014) Leiomodin-3 dysfunction results in thin filament disorganization and nemaline myopathy. *J Clin Invest* 124:4693–4708.
12. Cenik BK, et al. (2015) Severe myopathy in mice lacking the MEF2/SRF-dependent gene leiomodin-3. *J Clin Invest* 125:1569–1578.
13. Mymrikov EV, Seit-Nebi AS, Gusev NB (2011) Large potentials of small heat shock proteins. *Physiol Rev* 91:1123–1159.
14. Vos MJ, Kanon B, Kampinga HH (2009) HSPB7 is a SC35 speckle resident small heat shock protein. *Biochim Biophys Acta* 1793:1343–1353.
15. Mounier N, Arrigo AP (2002) Actin cytoskeleton and small heat shock proteins: How do they interact? *Cell Stress Chaperones* 7:167–176.
16. Wang K, Spector A (1996) Alpha-crystallin stabilizes actin filaments and prevents cytochalasin-induced depolymerization in a phosphorylation-dependent manner. *Eur J Biochem* 242:56–66.
17. Miron T, Wilchek M, Geiger B (1988) Characterization of an inhibitor of actin polymerization in vinculin-rich fraction of turkey gizzard smooth muscle. *Eur J Biochem* 178:543–553.
18. Krief S, et al. (1999) Identification and characterization of cvHsp. A novel human small stress protein selectively expressed in cardiovascular and insulin-sensitive tissues. *J Biol Chem* 274:36592–36600.
19. Cappola TP, et al. (2010) Common variants in HSPB7 and FRMD4B associated with advanced heart failure. *Circ Cardiovasc Genet* 3:147–154.
20. Matkovich SJ, et al. (2010) Cardiac signaling genes exhibit unexpected sequence diversity in sporadic cardiomyopathy, revealing HSPB7 polymorphisms associated with disease. *J Clin Invest* 120:280–289.
21. Stark K, et al. (2010) Genetic association study identifies HSPB7 as a risk gene for idiopathic dilated cardiomyopathy. *PLoS Genet* 6:e1001167.
22. Villard E, et al.; Cardiogenics Consortium (2011) A genome-wide association study identifies two loci associated with heart failure due to dilated cardiomyopathy. *Eur Heart J* 32:1065–1076.
23. Lahvic JL, et al. (2013) Small heat shock proteins are necessary for heart migration and laterality determination in zebrafish. *Dev Biol* 384:166–180.
24. Rosenfeld GE, Mercer EJ, Mason CE, Evans T (2013) Small heat shock proteins Hspb7 and Hspb12 regulate early steps of cardiac morphogenesis. *Dev Biol* 381:389–400.
25. Hayashi S, Lewis P, Pevny L, McMahon AP (2002) Efficient gene modulation in mouse epiblast using a Sox2Cre transgenic mouse strain. *Gene Expr Patterns* 2:93–97.
26. Chen JW, et al. (2006) Cardiomyocyte-specific deletion of the coxsackievirus and adenovirus receptor results in hyperplasia of the embryonic left ventricle and abnormalities of sinuatrial valves. *Circ Res* 98:923–930.
27. Moses KA, DeMayo F, Braun RM, Reecy JL, Schwartz RJ (2001) Embryonic expression of an Nkx2-5/Cre gene using ROSA26 reporter mice. *Genesis* 31:176–180.
28. Jiao K, et al. (2003) An essential role of Bmp4 in the atrioventricular septation of the mouse heart. *Genes Dev* 17:2362–2367.
29. Golenhofen N, Perng MD, Quinlan RA, Drenckhahn D (2004) Comparison of the small heat shock proteins alphaB-crystallin, MKBP, HSP25, HSP20, and cvHSP in heart and skeletal muscle. *Histochem Cell Biol* 122:415–425.
30. Zhou Q, Ruiz-Lozano P, Martone ME, Chen J (1999) Cypher, a striated muscle-restricted PDZ and LIM domain-containing protein, binds to alpha-actinin-2 and protein kinase C. *J Biol Chem* 274:19807–19813.
31. Zhou Q, et al. (2001) Ablation of cypher, a PDZ-LIM domain Z-line protein, causes a severe form of congenital myopathy. *J Cell Biol* 155:605–612.
32. Stewart JM, Levy HM (1970) The role of the calcium-troponin-tropomyosin complex in the activation of contraction. *J Biol Chem* 245:5764–5772.
33. Conover GM, Henderson SN, Gregorio CC (2009) A myopathy-linked desmin mutation perturbs striated muscle actin filament architecture. *Mol Biol Cell* 20:834–845.
34. Juo LY, et al. (2016) HSPB7 interacts with dimerized FLNC and its absence results in progressive myopathy in skeletal muscles. *J Cell Sci* 129:1661–1670.
35. Ono S (2010) Dynamic regulation of sarcomeric actin filaments in striated muscle. *Cytoskeleton* 67:677–692.
36. Heling A, et al. (2000) Increased expression of cytoskeletal, linkage, and extracellular proteins in failing human myocardium. *Circ Res* 86:846–853.
37. Tsukada T, et al. (2010) Leiomodin-2 is an antagonist of tropomodulin-1 at the pointed end of the thin filaments in cardiac muscle. *J Cell Sci* 123:3136–3145.
38. Gregorio CC, Weber A, Bondad M, Pennise CR, Fowler VM (1995) Requirement of pointed-end capping by tropomodulin to maintain actin filament length in embryonic chick cardiac myocytes. *Nature* 377:83–86.
39. Lin W, Yang Z, Lu Y, Zhao X (2014) Refined purification of large amounts of rat cvHsp/HspB7 and partial biological characterization in vitro. *Protein Pept Lett* 21:503–510.
40. Heacock CS, Bamburg JR (1983) The quantitation of G- and F-actin in cultured cells. *Anal Biochem* 135:22–36.
41. Fischer RS, et al. (2006) Tropomodulin 3 binds to actin monomers. *J Biol Chem* 281:36454–36465.
42. Yamashiro S, Speicher KD, Speicher DW, Fowler VM (2010) Mammalian tropomodulins nucleate actin polymerization via their actin monomer binding and filament pointed end-capping activities. *J Biol Chem* 285:33265–33280.
43. Lal AA, Korn ED (1985) Reinvestigation of the inhibition of actin polymerization by profilin. *J Biol Chem* 260:10132–10138.
44. Fowler VM, Dominguez R (2017) Tropomodulins and leiomodins: Actin pointed end caps and nucleators in muscles. *Biophys J* 112:1742–1760.
45. Wanger M, Keiser T, Neuhaus JM, Wegner A (1985) The actin treadmill. *Can J Biochem Cell Biol* 63:414–421.
46. Luther PK (2009) The vertebrate muscle Z-disc: Sarcomere anchor for structure and signalling. *J Muscle Res Cell Motil* 30:171–185.
47. Kappé G, et al. (2003) The human genome encodes 10 alpha-crystallin-related small heat shock proteins: HspB1-10. *Cell Stress Chaperones* 8:53–61.
48. Morrison LE, Whittaker RJ, Klepper RE, Wawrousek EF, Glembotski CC (2004) Roles for alphaB-crystallin and HSPB2 in protecting the myocardium from ischemia-reperfusion-induced damage in a KO mouse model. *Am J Physiol Heart Circ Physiol* 286:H847–H855.
49. Qiu H, et al. (2011) H11 kinase/heat shock protein 22 deletion impairs both nuclear and mitochondrial functions of STAT3 and accelerates the transition into heart failure on cardiac overload. *Circulation* 124:406–415.
50. Fang X, et al. (2017) Loss-of-function mutations in co-chaperone BAG3 destabilize small HSPs and cause cardiomyopathy. *J Clin Invest* 127:3189–3200.
51. Vos MJ, et al. (2010) HSPB7 is the most potent polyQ aggregation suppressor within the HSPB family of molecular chaperones. *Hum Mol Genet* 19:4677–4693.
52. Liao WC, Juo LY, Shih YL, Chen YH, Yan YT (2017) HSPB7 prevents cardiac conduction system defect through maintaining intercalated disc integrity. *PLoS Genet* 13:e1006984.
53. National Research Council (2011) *Guide for the Care and Use of Laboratory Animals* (National Academies Press, Washington, DC), 8th Ed.
54. Liang X, et al. (2005) PINCH1 plays an essential role in early murine embryonic development but is dispensable in ventricular cardiomyocytes. *Mol Cell Biol* 25:3056–3062.
55. Stroud MJ, et al. (2017) Nesprin 1α2 is essential for mouse postnatal viability and nuclear positioning in skeletal muscle. *J Cell Biol* 216:1915–1924.
56. Arita Y, et al. (2014) Myocardium-derived angiopoietin-1 is essential for coronary vein formation in the developing heart. *Nat Commun* 5:4552.
57. Fang X, et al. (2016) Adipocyte-specific loss of PPARγ attenuates cardiac hypertrophy. *JCI Insight* 1:e89908.
58. Bogomolovas J, Simon B, Sattler M, Stier G (2009) Screening of fusion partners for high yield expression and purification of bioactive viscotoxins. *Protein Expr Purif* 64:16–23.
59. Huang C, et al. (2003) Characterization and in vivo functional analysis of splice variants of cypher. *J Biol Chem* 278:7360–7365.
60. Gregorio CC, Fowler VM (1995) Mechanisms of thin filament assembly in embryonic chick cardiac myocytes: Tropomodulin requires tropomyosin for assembly. *J Cell Biol* 129:683–695.
61. Zhou W, et al. (2007) Modulation of morphogenesis by noncanonical Wnt signaling requires ATF/CREB family-mediated transcriptional activation of TGFbeta2. *Nat Genet* 39:1225–1234.
62. Mu Y, et al. (2015) Cypher and Enigma homolog protein are essential for cardiac development and embryonic survival. *J Am Heart Assoc* 4:e001950.